Electronic Supplementary Information (ESI) for

Organic Acid Evaporation Kinetics From Aqueous Aerosols: Implications for Aerosol Buffering Capacity in the Atmosphere

Kyle J. Angle, Christopher M. Nowak, Vicki H. Grassian*

Supplementary Discussion Points

Discussion Point S1. Lactic acid Raman peak assignments.

The peak at 750 cm^{-1} is assigned to the O-C-O stretch of the acidic form. This peak is weak in the aerosol-phase spectrum. As discussed in the text, the peaks at 830 and 856 cm^{-1} are from the C-COOH and C-COO^- stretches, and the colorblind reader can use these to distinguish the spectra shown in Fig. 2a. For both forms, there is a peak at 875 cm^{-1} which we assign to C-$COH_{alcohol}$. The peaks at 980 and 1050 cm^{-1} are the sulfate and nitrate standards, respectively. The 1088 cm^{-1} peak is assigned to the alcohol O-H stretch and is weak in the aerosol phase. The strong peak at 1420 cm^{-1} is assigned to the COO^- symmetric stretch and is therefore characteristic of the conjugate base. The 1456 cm^{-1} peak is assigned to the CH_3 asymmetric stretch and is present for both forms. Finally, the 1730 cm^{-1} peak is attributed to C=O for lactic acid, although the peak is weaker and more diffuse in the aerosol phase, meaning it can only be used qualitatively in Fig. 2b to confirm evaporation of lactic acid.

Discussion Point S2. Butyric acid coalescence experiment.

Aerosol-phase experiments with butyric acid are challenging because the acid poorly nebulizes from the nebulizer that creates aerosols of the appropriate size for the Biral AOT instrument used. This is because the nebulizer is optimized for medicinal purposes involving more dilute (and hence less viscous) aqueous solutions. As a result, we found more success nebulizing solutions that contained 1 m sodium butyrate. The aerosols experience acidification upon nebulization, resulting in droplets of lower pH (as indicated by the spectra) compared to the solution they were nebulized from. The extent of this acidification varies due to factors such as initial pH, but in our case, we are able to estimate the final pH using the peaks at 1414 and 1453 cm^{-1}. Once optically trapped, butyric acid could be acidified via coalescence with HCl aerosols. A representative result is given in Fig. S6. With the pH-dependence of the collection of peaks at 1414 and 1453 cm^{-1} established in Fig. 5a, one would expect the ratio to shift toward a lower pH with consecutive coalescence events. Instead, however, it can be seen that these peaks decrease in intensity and eventually fall below the limit of detection by the last coalescence. Importantly, the nitrate peak remains at a relatively constant intensity, indicating this is not due to dilution. Instead, the butyric acid that is formed by coalescence rapidly evaporates from the aerosol, leaving behind a particle with a similar pH and a lower organic fraction. This highlights the unique type of titration possible for particles containing volatile organic acids surrounded by a low concentration of that acid in the gas phase. We also note that this experiment was performed immediately following the experiment shown in Fig. 5b, so it is possible that buildup of butyric acid in the AOT chamber slowed the net evaporation rate.

Discussion Point S3. Starting with lactic acid compared to starting with lactate.

We have proposed the possibility of superbuffering in aerosols when organic acids evaporate from aerosols. Specifically, the new mechanism we have presented posits that when the conjugate base of an organic acid is protonated via titration, the organic acid then evaporates quickly, removing the acidity. In the manuscript, we focused only on the rate of the evaporation of the organic acid. To have data for the full process, we now discuss the rate when the acidification step is included. Although acid-base chemistry is known to be very fast, phenomena such as concentration gradients could impact reaction rates.[4] To test whether starting with the conjugate base would slow down evaporation, we performed some experiments by trapping aerosols composed of lactic acid and others by trapping sodium lactate and acidifying the aerosol with HCl. For these acidification experiments, the same approach was applied as described in the main text, and the rate at 95% confidence is $1.6 \pm 0.6 * 10^{-2}$ s^{-1}. The large confidence interval is due to variability between experiments, since enrichment factors apply to both the initial aerosol and the coalescing aerosol, as well as variability in the size of the aerosol that coalesces with the trapped aerosol. Nevertheless, the titration (initial lactate aerosol) 95% confidence interval encompasses the non-titration (initial lactic acid aerosol) 95% confidence interval of $1.2 \pm 0.3 * 10^{-2}$ s^{-1}. This is a key point because it indicates that the titration step does not impact the evaporation rate. The utility of this result is that other experiments can be performed by trapping an aerosol that initially contains an acid and omitting the acidification step, which reduces sources of experimental variability.

Supplementary Figures (Figure S1-S9).

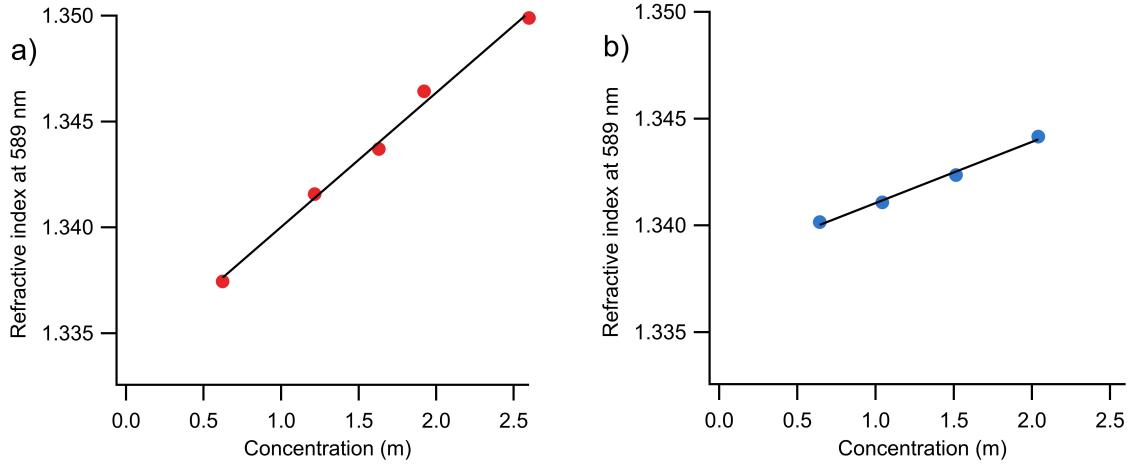

Fig. S1. Bulk refractive index measurements for (a) lactic acid and (b) lactate. The fits are (0.0063 ± 0.0009)x + (1.334 ± 0.002) with R^2 = 0.99 and y = (0.0029 ± 0.0008)x + (1.338 ± 0.001) with R^2 = 0.99, respectively. Note that the intercept of the fit line is higher for lactate due to the salt created from neutralizing lactic acid with NaOH.

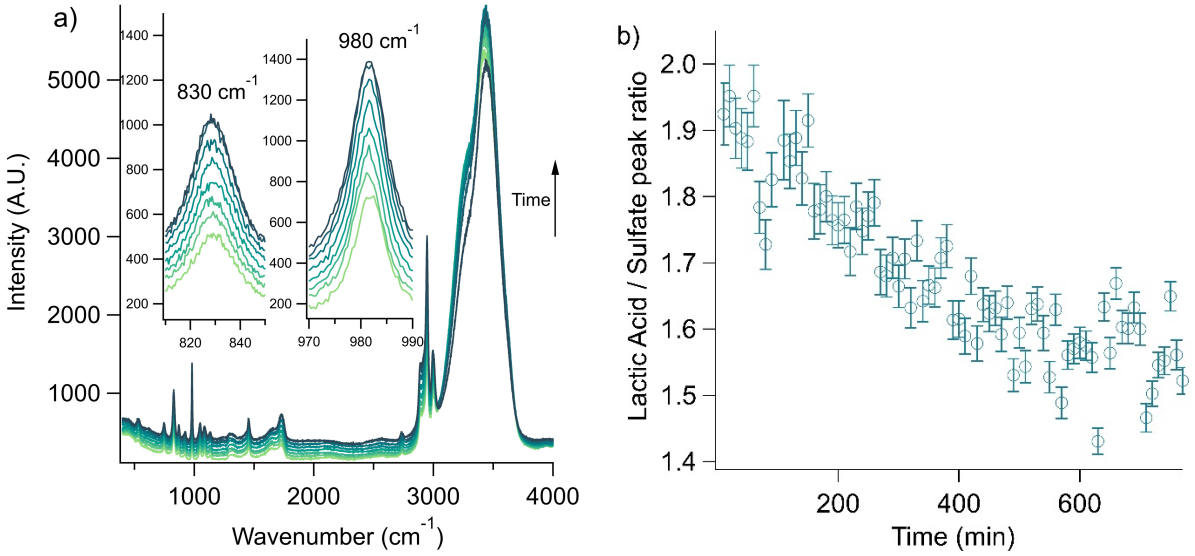

Fig S2. (a) Bulk phase spectra of lactic acid evaporation offset for clarity. Spectra show 100 minute increments (bottom to top) with the inset focusing on showing the increase in the lactic acid C-COOH band and sulfate internal standard band due to water evaporation. (b) The ratio of these peak areas over time. The gradual decline is used as a measure of lactic acid evaporation.

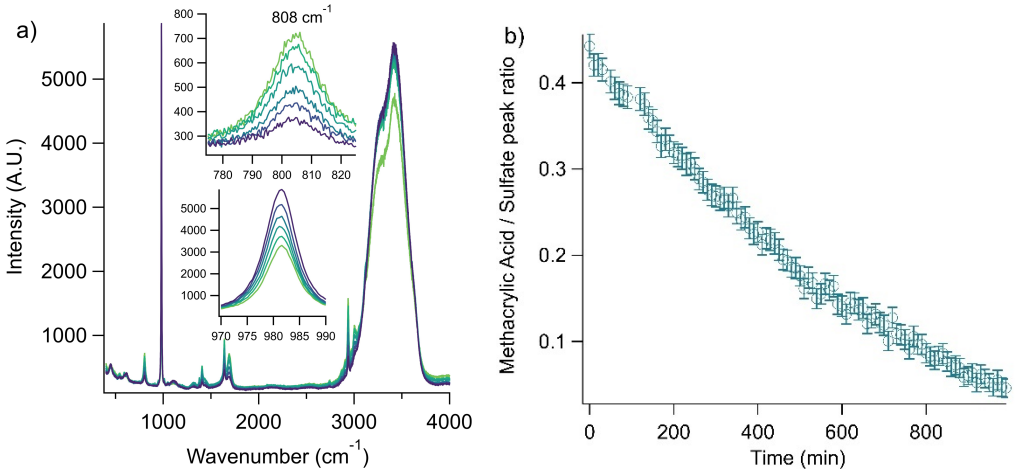

Fig. S3. (a) Bulk phase spectra of methacrylic acid evaporation showing 200 minute increments (from green to violet). No offset was used. The insets show how methacrylic acid (808 cm^{-1}) decreases from evaporation even as sulfate (980 cm^{-1}) increases due to concentration from water evaporation. (b) The ratio of these peaks over time used to calculate evaporation rate.

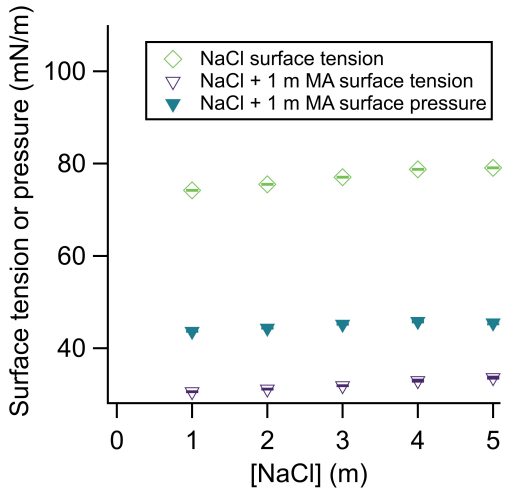

Fig. S4. Surface pressure of 1 m methacrylic acid solutions (filled triangles). Data points are obtained by subtracting the surface tension of a solution with 1 m methacrylic acid and the given [NaCl] from the surface tension of a solution containing only the NaCl adjusted to the same pH as the methacrylic acid solutions (pH 2.3) with 6 M NaCl. The slight decrease from 4 to 5 m NaCl may be due to combinations of self-polymerization of methacrylic acid and the high ionic strength medium. Significantly less change in surface pressure with [NaCl] is observed compared to lactic acid (Fig. 3b), implying salting-out is a less important phenomenon for methacrylic acid. Error bars, smaller than the symbols, show standard deviation of replicates.

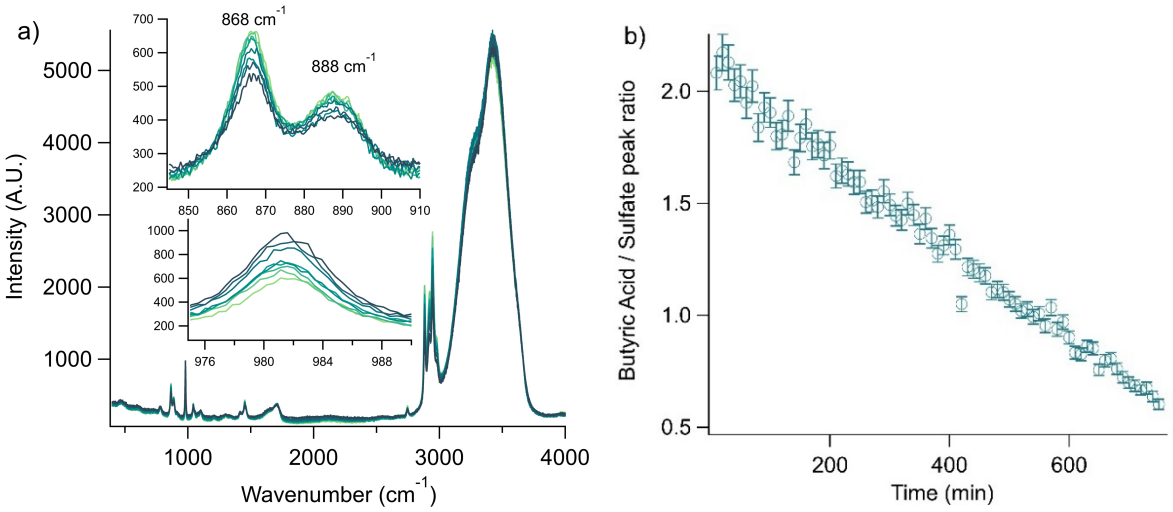

Fig. S5. (a) Bulk spectra of butyric acid evaporation overlayed, with the color progression from green to violet showing spectra in 100-minute intervals. The top inset shows a loss of butyric acid over time while the bottom inset shows an increase in sulfate due to concentration. (b) The ratio of the left butyric acid peak (868 cm^{-1}) vs the sulfate peak over time used to calculate evaporation rate.

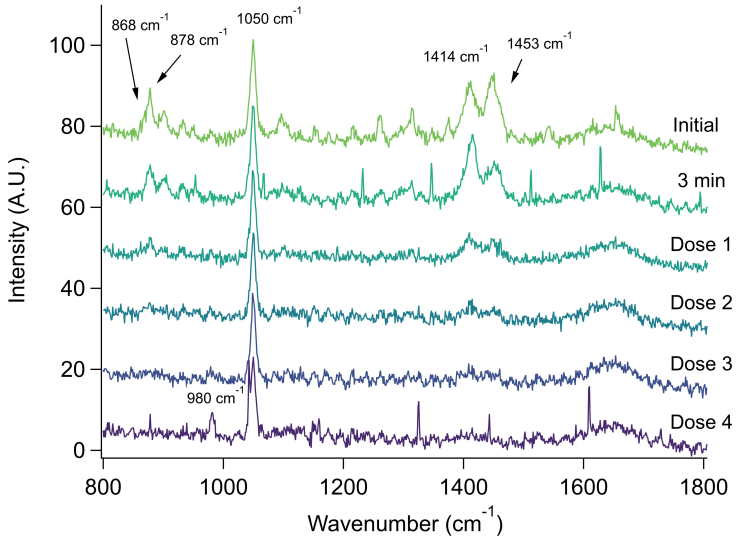

Fig. S6. Aerosol-phase experiment showing the loss of butyric acid from titration by droplet coalescence. A 1 m butyrate bulk solution at pH 5 was nebulized and spectra were recorded (labeled "Initial"). Butyric acid was allowed to evaporate for three minutes ("3 min"), raising the pH of the system via loss of the acid as can be observed by the ratio of the 1414 and 1453 cm^{-1} peaks. Then a series of coalescences with small 1 m HCl aerosols (see an approximate size distribution in Fig. S5a of Angle *et al.*[1]) were performed. Rather than lowering the pH (which would be seen as an increase in the intensity of the 1453 cm^{-1} peak), both the 1414 and 1453 cm^{-1} peaks decrease with each coalescence. Eventually, butyric acid and butyrate are completely removed from the aerosol phase. Note the sharp frequencies correspond to WGMs and a small quantity of sulfate was included in the HCl to confirm coalescence was occurring (see the 980 cm^{-1} band in "Dose 4") while $NaNO_3$ (1050 cm^{-1}) was only included in the original aerosol to confirm that decreases in butyric acid and butyrate peaks were not due to dilution.

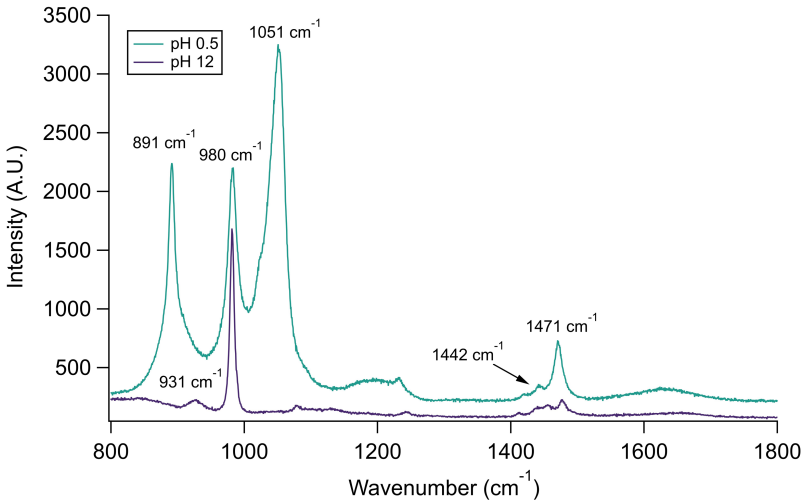

Fig. S7. Confocal spectra of DMA (pH 12) and DMAH (pH 0.5). The 980 cm^{-1} band corresponds to sulfate, the internal standard. The C-N-C symmetric stretch (ν_s) at 931 cm^{-1} is the unique identifier of the neutral amine, as the peaks at 1442 and 1471 cm^{-1} (C-H stretches) are present in both spectra and therefore not useful for identifying an individual form of the molecule.

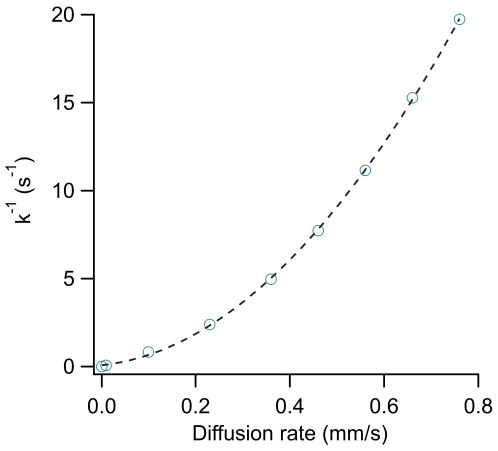

Fig S8. Sensitivity analysis for calculated evaporation rate constant at different diffusion rates. The top right data point corresponds to a rate equal to the diffusion coefficient with a 100% probability of escaping the aerosol upon arriving at the aerosol-air interface. Simulations were performed using 10^5 particles, as it was found that increasing the particles to 10^6 only changed k by 0.12% while greatly increasing computing cost. Data points fit $y = (30.3 \pm 0.6)x^2 + (2.8 \pm 0.5)x + (0.08 \pm 0.07)$ with $R^2 = 0.999$.

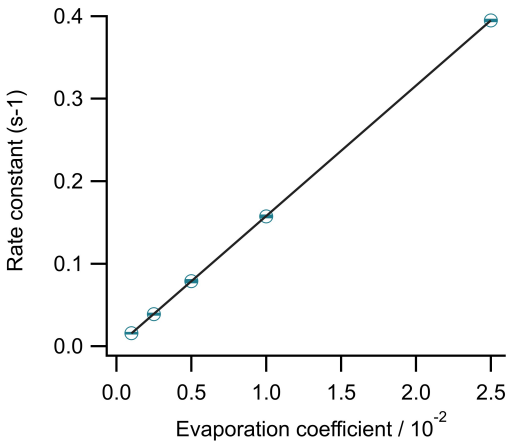

Fig. S9. Results from varying an evaporation coefficient, sometimes discussed in conjunction with mass accommodation coefficients (α). Values of α near unity have been calculated for acids of varying structure.[2] Elsewhere evaporation coefficients as low as 10^{-4} have been reported, although further analysis shows that values < 0.01 are unlikely, and convoluting effects of non-ideality may impact the applicability of this analysis.[3,4] At 95% confidence, data fit the equation y = (15.81 ± 0.05)x – (0.0004 ± 0.0006) with R^2 = 0.999.

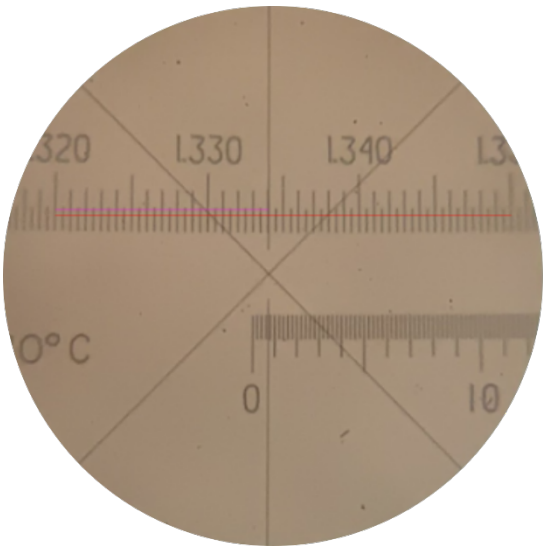

Fig. S10. Example refractometer reading. The red line (bottom horizontal line) is drawn to determine the number of pixels in 0.03 refractive index units. The number of pixels in the fuchsia (top horizontal line) can then be used to determine the number of refractive index units to add to 1.320 to get the sample refractive index.

Supplementary Table.

Table S1. E-AIM model III pH calculation inputs and calculated pH results. All calculations were run at an RH of 0.80. The pH_m value was obtained using Equation S1.[5] Blank cells correspond to values of 0.

Na^+	Cl^-	H^+	SO_4^{2-}	NO_3^-	Lactic Acid	Methacrylic Acid	pH_m
1	1				1		1.48
2	2				1		1.56
3	3				1		1.62
4	4				1		1.67
5	5				1		1.71
0.5	0.5				2		1.43
1.5	1.5				2		1.46
1.34			0.67			0.67	2.52

$$pH_m = -\log(x_H * f_H) - 1.74 \quad \text{(S1)}$$

Here, pH_m is molality-based pH, x_H is the mole fraction of H^+, f_H is the mole fraction activity coefficient of H^+, and 1.74 is the conversion from mole-fraction to molality-based pH.

ESI References.

(1) Angle, K. J.; Crocker, D. R.; Simpson, R. M. C.; Mayer, K. J.; Garofalo, L. A.; Moore, A. N.; Mora Garcia, S. L.; Or, V. W.; Srinivasan, S.; Farhan, M.; Sauer, J. S.; Lee, C.; Pothier, M. A.; Farmer, D. K.; Martz, T. R.; Bertram, T. H.; Cappa, C. D.; Prather, K. A.; Grassian, V. H. Acidity across the Interface from the Ocean Surface to Sea Spray Aerosol. *Proc. Natl. Acad. Sci.* **2021**, *118* (2), e2018397118.

(2) Julin, J.; Winkler, P. M.; Donahue, N. M.; Wagner, P. E.; Riipinen, I. Near-Unity Mass Accommodation Coefficient of Organic Molecules of Varying Structure. *Environ. Sci. Technol.* **2014**, *48* (20), 12083–12089.

(3) Cappa, C. D.; Wilson, K. R. Evolution of Organic Aerosol Mass Spectra upon Heating: Implications for OA Phase and Partitioning Behavior. *Atmos. Chem. Phys.* **2011**, *11* (5), 1895–1911.

(4) Saleh, R.; Shihadeh, A.; Khlystov, A. Determination of Evaporation Coefficients of Semi-Volatile Organic Aerosols Using an Integrated Volume-Tandem Differential Mobility Analysis (IV-TDMA) Method. *J. Aerosol Sci.* **2009**, *40* (12), 1019–1029.

(5) Jia, S.; Wang, X.; Zhang, Q.; Sarkar, S.; Wu, L.; Huang, M.; Zhang, J.; Yang, L. Technical Note: Comparison and Interconversion of pH Based on Different Standard States for Aerosol Acidity Characterization. *Atmos. Chem. Phys.* **2018**, *18* (15), 11125–11133.